

HIAM: Hidden Node and Interference Aware Routing Metric for Multi-channel Multi-radio Mesh Networks

Deema Hammash
Korea Advanced Institute of
Science and Technology
Daejeon, South Korea
deema@kaist.ac.kr

Myungchul Kim
Korea Advanced Institute of
Science and Technology
Daejeon, South Korea
mck@kaist.ac.kr

Ben Lee
Oregon State University
OR 97331, USA
benl@eecs.oregonstate.edu

Sungwon Kang
Korea Advanced Institute of
Science and Technology
Daejeon, South Korea
sungwon.kang@kaist.ac.kr

Younghee Lee
Korea Advanced Institute of
Science and Technology
Daejeon, South Korea
yhlee@cs.kaist.ac.kr

Dongman Lee
Korea Advanced Institute of
Science and Technology
Daejeon, South Korea
dlee@cs.kaist.ac.kr

ABSTRACT

In wireless mesh networks, throughput degrades drastically as the network size grows mainly due to the hidden node problem and carrier sense interference. These phenomena can be avoided in multi-channel, multi-radio mesh networks by choosing a path consisting of channels in which the two problems can be mitigated. This paper proposes a new routing metric, the Hidden node and Interference Aware routing Metric (HIAM), which considers both problems when choosing paths. The effect of the hidden node problem for a path is represented by estimating the packet transmission time with respect to the number of collisions that can occur due to hidden nodes. The effect of carrier sense interference for a path is represented by estimating the packet transmission time with respect to inter-flow and intra-flow interference. Our simulation results show that HIAM results in significantly higher routing stability and throughput, and lower control packet overhead than the existing methods.

Categories and Subject Descriptors

C.2.2 [Computer-Communication Networks]: Network Protocol—*routing protocols*

General Terms

Measurement, Design, Experimentation

Keywords

hidden node, interference, multi-channel, multi-radios.

1. INTRODUCTION

Permission to make digital or hard copies of all or part of this work for personal or classroom use is granted without fee provided that copies are not made or distributed for profit or commercial advantage and that copies bear this notice and the full citation on the first page. To copy otherwise, to republish, to post on servers or to redistribute to lists, requires prior specific permission and/or a fee.

ICUIMC(IMCOM)'13, January 17-19, 2013, Kota Kinabalu, Malaysia.
Copyright 2013 ACM 978-1-4503-1958-4 ...\$15.00.

Wireless Mesh Networks (WMNs) have received a great deal of attention in recent years due to their low up-front costs, easy network maintenance, robustness, and reliable service coverage [1]. However, throughput in a WMN drastically degrades as the size of network grows [2, 3]. This degradation is caused by two major problems [2, 3, 4, 5]. The first problem is due to *interference* among nodes within the carrier sense range of one another. This may occur between two nodes on a path towards a common destination, called *intra-flow interference*, or among nodes on adjacent paths involved in different flows, called *inter-flow interference*. The second problem is the *hidden node effect*, which occurs when two senders out of each other's carrier sense range are transmitting in overlapping time spans, and one of the sender's receiver is in the carrier sense range of both senders. A study in [2] showed that a single chain of nodes using the same channel and Request To Send (RTS)/Clear To Send (CTS) is able to utilize only a quarter of the channel capacity. Moreover, if this chain were to be combined with other adjacent chains, the channel utilization drops to 1/12 [2]. Studies presented in [3, 5, 16, 19] showed that the hidden node problem has a more detrimental effect on performance, and a study in [6] showed that transmission failures due to the hidden node problem are two orders of magnitude higher than transmission failures caused by carrier sense interference.

Employing multi-channel, multi-radio has been shown to be an effective approach to increase network capacity [8, 9, 10]. However, most of the past research on routing metrics for multi-channel, multi-radio do not explicitly consider the hidden node problem, and instead focuses on other factors, such as inter- and intra-flow interference. De Couto *et al.* proposed a routing metric called *Expected Transmission Count* (ETX) [7], which uses link loss ratio as a basis for choosing a path with the best link quality. However, ETX does not deal with the hidden node effect appropriately [10]. Draves *et al.* proposed the *Weighted Cumulative Expected Transmission Time* (WCETT) metric that incorporates link loss ratio, link bandwidth, and channel diversity information of a path into the metric. However, WCETT does not consider the hidden node problem in its routing metric explicitly [10]. The same applies to many other metrics that only consider inter-flow or intra-flow interference,

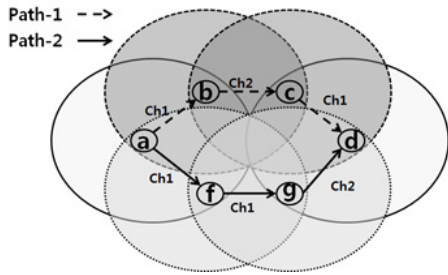


Figure 1: Hidden node problem and carrier sense interference.

such as *Interference aware Resource Usage* (IRU) [17].

There are few proposed metrics in the literature that consider the hidden node effect in multi-channel, multi-radio wireless networks [9, 10]. However, the work presented in [9] used a simplified estimation of the number of collisions due to hidden nodes, where the probability of hidden nodes transmission were only considered, neglecting the probability of affected node transmission. This can make it unable to recognize paths with fewer number of hidden node collisions. In addition, carrier sense interference was not considered in its path selection process. In Path Predicted Transmission Time (PPTT) metric presented in [10], the estimation of number of collisions due to hidden nodes and carrier sense interference incurs control packet overhead to gather the necessary information, and the hidden node problem was not given the highest priority during the path selection resulting in choosing paths with lower throughput. Furthermore, both metrics were designed only for the scenarios in which the carrier sense and transmission ranges are equal.

This paper proposes a new routing metric, called *Hidden node and Interference Aware routing Metric* (HIAM) for multi-channel, multi-radio WMNs, which takes into account inter-flow interference, intra-flow interference, and the hidden node problem to choose paths with the highest throughputs. Our simulation study using QualNet [12] simulator shows that HIAM results in significantly higher throughput and routing stability, and lower control packet overhead than ETX, WCETT, IRU, or PPTT.

The specific contributions of this paper are as follows: (i) The hidden node problem is explicitly considered in the proposed metric using an analytical model; (ii) the effect of carrier sense interference is incorporated into the proposed metric using enhanced ETX and WCETT; (iii) a routing protocol using the metric is proposed; and (iv) the proposed HIAM and its accompanying routing protocol are validated using simulation.

This paper is organized as follows: Sec. 2 discusses the performance issues in WMNs; Sec. 3 presents the related work; The proposed HIAM is presented in Sec. 4; Sec. 5 presents a HIAM-based routing protocol followed by a performance evaluation in Sec. 6; Finally, conclusion and future work are discussed in Sec. 7.

2. PERFORMANCE ISSUES IN WMNS

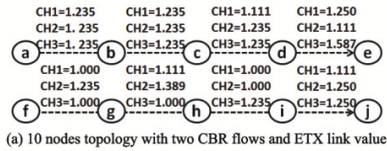
The *hidden node* (HN) problem and *carrier sense interference* (CSI), and their effect on throughput degradation are illustrated in Fig. 1. For simplicity assume that transmission range (Tx_{range}) and carrier sense range (CS_{range}) are equal. In Path-1, when node c communicates to node d ,

node b senses the channel to be busy while node a senses the channel to be idle, since node c is inside the carrier sense range (CS_{range}) of node b but outside the CS_{range} of node a . If node a starts transmitting to node b while node c is still transmitting to node d , node b will continue to sense the channel as busy, and it will not receive the packet from node a . As a result, node b will not return an ACK to node a . Node a may then time out and double the contention window size for retransmission later, while Node c transmission is not affected at all [3]. Therefore, node c is a *hidden node* (HN) for the *affected node* (AffN) a , and link cd is referred to as a *hidden link* (HL) for the *affected link* (AffL) ab .

On the other hand, in Path-2, node f communicates to node g . Since node f is within the CS_{range} of node a , node a cannot transmit to node f or node b while node f transmits, which forces node a to defer any transmissions for a back-off interval picked randomly from the contention window. This causes delays and collisions in case of simultaneous transmission between nodes just finished counting down their back-off interval. In this case, node f is referred to as a *carrier sense node* (CSN) (or interfering node) for the node a , and link fg is referred to as a *carrier sense link* (CSL) (or interfering link) for both links, af , and ab .

Most of the existing research on multi-channel, multi-radio wireless routing metrics [7, 8] focus on finding a path with the least amount of CSI. This is done by choosing a path with the highest channel diversity among nodes that reside within the CS_{range} of each other. However, these metrics may inadvertently favor paths with HNs over paths with CSI, as illustrated using examples and simulation results in Sec. 3. In order to compare the effects of the HN problem (i.e., as in Path-1) versus CSI (i.e., as in Path-2) on throughput, the two paths shown in Fig. 1 were analyzed using simulation (see Sec. 6) based on the following assumptions: no RTS/CTS, Constant Bit Rate (CBR) traffic with a flow rate of 1.4 Mbps, and two channels per node based on IEEE 802.11b radios. The simulation results show that the HN problem causes greater throughput degradation than CSI. Path-2 achieved 2x higher throughput (i.e., Path-1=0.305 Mbps, Path-2=0.675 Mbps), and 1.5x lower delay than Path-1.

There are two interrelated reasons behind the large throughput degradation due to the HN problem [3, 4, 5]. The first reason is that collisions on an AffL cause high packet drop rate. For example, in Path-1 for Fig. 1, if node a starts transmitting to node b while node c is transmitting to node d , node b will drop the packet and node a will perceive this as a collision at node b . Node a will know about this collision as soon as the acknowledgement (ACK) time-out expires. It will then randomly select a backoff interval from the contention window. This backoff interval will be counted down by one time slot whenever it senses that the channel is idle. However, since node a is not aware of the transmission of node c , it will sense the channel as being idle over the entire time (unless one of the CSNs of node a is using the channel). Afterwards, node a will retransmit the packet. However, this packet will also collide with if node c is still transmitting. Such collisions will cause packets to be dropped and the link to be broken when the IEEE 802.11 MAC retransmission limit is exceeded. The second reason is frequently broken links. When a link is considered broken the current route to the destination is disabled. This causes all the packets waiting in the queue to be dropped, and a



Flow	Path	HN	ETX_{path}	WCETT
Flow1	P1={a-CH1,b-CH2,c-CH1,d-CH2}	Y	4.692	45.747
	P2={a-CH1,b-CH2,c-CH2,d-CH1}	N	4.955	48.361
	P3={a-CH1,b-CH1,c-CH2,d-CH2}	N	4.816	47.359
Flow2	P1={f-CH2,g-CH3,h-CH3,i-CH3}	Y	4.720	53.333
	P2={f-CH2,g-CH3,h-CH2,i-CH1}	Y	4.346	42.777
	P3={f-CH2,g-CH3,h-CH1,i-CH2}	N	4.485	45.306

(b) ETX and WCETT selected routing paths

Figure 2: ETX example.

new route discovery will be initiated. This new route will face the same outcome as the previous one due to HNs. In addition, frequent broadcasting of route discovery packets will incur high control overhead on the network, forcing other flows to defer their packets in their queues. This in turn causes queues to overflow and increases the chances of collisions due to higher contention over the channel.

In contrast, the chances of collisions due to CSI are lower because each node can hear the transmission of other nodes within its CS_{range} , causing collisions only when two nodes start transmitting at the same time [14]. Nevertheless, the effect of CS_{range} is still significant [2]. Especially in networks with high traffic load, the contention rates increases and the probability of concurrent transmissions between contending nodes increases as well. Therefore, both problems need to be considered in the path selection process with a higher weight given to the HN problem.

3. RELATED WORK

A significant amount of research exists on routing metrics for multi-channel, multi-hop WMNs. However, most of the existing studies address either CSI or load balancing and do not consider the HN problem explicitly. De Couto *et al.* proposed the ETX metric for link quality, which is the number of predicted data transmissions required to send a packet over a link including retransmissions [7]. However, ETX_{path} metric ($\sum_{ij \in Path} ETX_{ij}$) does not consider link bandwidth and channel-diversity in the path selection process [8]. In addition, ETX does not properly distinguish between a path that has HNs and another that is HN-free [10] as illustrated in Fig. 2-a using 10 nodes topology with 802.11b radios, and Tx_{range} of 370m and CS_{range} of 670m, which are similar to the parameters of Lucent ORiNOCO wireless cards in an outdoor environment. The distance between nodes is 345m. Two sender/receiver pairs are used: node *a* and node *e* (Flow 1), node *f* and node *j* (Flow 2). Flow 1 starts at the 15th second, while Flow 2 starts at the 25th second. Each node is equipped with three radios and three channels, each radio is fixed to a specific channel (i.e., CH1, CH2, and CH3), and ETX metric was placed in AODV routing protocol. The ETX values shown for links between nodes {*a*, *b*, *c*, *d*, *e*} are the result of the first measurement window (i.e., 10 seconds), during which no flows were active. On the other hand, the ETX values shown for links between nodes {*f*, *g*, *h*, *i*, *j*} are the result of the second measurement

window, during which Flow 1 was active. The protocol waits for three RREQ packets then chooses the best path based on ETX metric. Fig. 2-b shows the three candidate paths (i.e., P1, P2, and P3) reached the destination node, and their corresponding ETX_{path} metric value. Note that Flow 1 has two paths without HNs, P2 and P3. However, ETX_{path} chooses P1 (i.e., P1 has the lowest ETX_{path} value) for Flow 1, which is a path with two HNs: node *c* and *d*. On the other hand, Flow 2 has two paths with HN problem, P1 (i.e., node *i* is HN for node *g*) and P2 (i.e., node *h* is HN for node *f*). However, ETX_{path} favors P2 for Flow 2 over the optimal path, P3, which have no HN problem or CSI. Despite that in some cases the ETX link value can reflect the HN effect, yet the ETX_{path} metric ($\sum_{ij \in Path} ETX_{ij}$) cannot recognize a path with a HN problem due to three main reasons: First, the ETX_{path} metric does not explicitly consider the hidden node problem in the path selection process. Second, the ETX weakly reflects the HN problem, because ETX can reflect current link condition based on the existing traffics in the network. Therefore, in routing selection stage, the coming traffic is not injected into the network yet so the ETX values cannot account for the effect of idle HNs in a path as shown in Fig. 2, which causes wrong routing selection [10]. This brings the need for an analytical model that can predict the number of HN collisions. Third, as admitted in the ETX paper [7, 11], heavy load causes the MAC protocol to become extremely unfair, distorting the probe-based measurements. Thus, ETX might not accurately estimate the link delivery probabilities and accordingly result in sub-optimal paths. Furthermore, ETX value does not properly reflect dynamic changes in link quality due to the large measurement window (i.e., 10 seconds) used to calculate ETX value per link. Therefore, routes that got broken due to excessive collisions during that window, are not reflected immediately in the ETX value, which forces the new routes to be selected based on the same old ETX link values that were used to select the broken routes. This causes wrong routing selection. On the other hand, Draves *et al.* proposed WCETT [8], which combines ETX with link bandwidth to produce the estimated packet transmission time and *explicitly* considers CSI by taking into account channel diversity within a path. However, WCETT has some drawbacks. First, WCETT does not explicitly take into account paths with HNs and inter-flow interferences [10]. In fact, our simulations shows that WCETT may favor paths with HNs over HN free paths, as illustrated in the example shown in Fig. 2. In this example the same process used in analyzing ETX is used to analyze WCETT. Note that for Flow 1 WCETT favors P1 over two HN free paths, and for Flow 2 WCETT favors P2 over the HN free and CSI free path, P3. In P3 both links *ij* and *fg* are using the same channel (i.e., CH2), however, link *ij* is out of the CS_{range} for both links *fg* and *gh*. The second problem in WCETT, is the inadequacy in reflecting the actual channel-diversity of a route [10]. This is because WCETT considers all the links that use the same channel in a path as interfering links, regardless of whether these links are in the CS_{range} of each other or not. Thus, WCETT in some cases is unable to recognize paths with better channel diversity as shown in Fig. 2-b. WCETT favors P3 over P2 for Flow 1 (i.e., WCETT values for P2 = 48.361, and P3 = 47.359), keeping in mind that P3 has 2 pairs of interfering links, (*ab*, *bc*) and (*cd*, *de*), which are using CH1 and CH2 respectively. On the other hand, P2 has

one pair of interfering links, (bc, cd) . Yang *et al.* proposed IRU to solve some of the problems in WCETT by considering both intra-flow and inter-flow interferences. But, it does not consider bottleneck channels and the HN problem.

Metrics that consider the HN effect are discussed in [9] and [10]. Sangiamwong *et al.* proposed the hidden node aware metric designed for the 802.11s standard and specifically addressed VoIP applications [9]. This metric predicts the number of collisions due to HNs by considering only the HN transmission time ratio but neglects the transmission time of the AffN. Thus, it misses a crucial point in the causes of HN collisions, which is that a collision can only occur during concurrent or overlapped transmission between a HN and an AffN. Their metric overestimates the number of HN collisions, consequently avoiding paths with high estimated collisions even though they may actually have a lower number of collisions than others. Furthermore, in the case of multiple HNs for a single AffN, it assumed that all HN transmissions are independent. This assumption is not applicable when such multiple HNs are residing within each others CS range, which produces incorrect estimations. In addition, the CSI was not considered in its path selection process.

On the other hand, Yin *et al.* proposed the Path Predicted Transmission Time (PPTT) that mainly chooses paths with the lowest end-to-end delay as a crucial requirement for real-time traffic [10]. This metric uses an analytical model to predict the effect of CSI, and the HN problem on packet transmission time along a path. The required information for this analytical model is collected using new periodic control messages in addition to Route Request (RREQ) and Route Reply (RREP) packets, which causes control packet overhead problems and wastes bandwidth. Furthermore, this metric like the one in [9] were designed only for scenarios in which the CS_{range} and Tx_{range} are equal.

In contrast, our proposed routing metric is designed to work with any CS_{range} and Tx_{range} , using the Network Discovery phase in our proposed routing protocol, nodes within CS_{range} and Tx_{range} are identified and marked. Our metric provides good predictions on the number of HN collisions with minimal control packet overhead due to three main reasons: First, our analytical model requires exchanging few parameters between nodes using Hello packets and RREQs. Second, Hello packet broadcast overhead is reduced using *grouping method* explained in Section 4.2 (i.e., Hello packet size may reach up to 1.2x smaller than PPTT periodic control packet size). Third, route discovery overhead is reduced using the *early elimination scheme* explained in Section 4.3. Furthermore, unlike PPTT, HIAM uses both active probing and analytical model to reflect the HN effect and CSI. In addition, a higher weight is given to the HN effect in the path selection process, which leads to higher throughput. HIAM also alleviates problems in ETX and WCETT by enhancing ETX to reflect dynamic link quality changes every second with moving averages for delivery ratios, and enhancing WCETT to consider inter-flow interference and the channel diversity problem.

4. THE PROPOSED ROUTING METRIC: HIAM

The Hidden node and Interference Aware routing Metric

(HIAM) is given by

$$HIAM = \beta \times CEPTT^{HN} + (1 - \beta) \times WCEPTT^{CS}, \quad (1)$$

where β is a tunable parameter ($0 \leq \beta \leq 1$). *Cumulative Expected Packet Transmission Time* ($CEPTT^{HN}$) estimates the effect of HNs on or adjacent to a path, and *Weighted CEPTT^{CS}* ($WCEPTT^{CS}$) estimates the effect of CSI on a path. The details of $CEPTT^{HN}$ and $WCEPTT^{CS}$ are explained in the following two subsections.

4.1 Cumulative Expected Packet Transmission Time with Hidden Nodes ($CEPTT^{HN}$)

$CEPTT^{HN}$ over a path p is estimated as follows:

$$CEPTT^{HN} = \sum_{ij \in p} EPTT_{ij}^{HN}, \quad (2)$$

where $EPTT_{ij}^{HN}$ represents the *expected packet transmission time* for a single packet over a link ij , including retransmissions caused by collisions due to all HNs, and is given by

$$EPTT_{ij}^{HN} = PTT_{ij} \times Col_{ij}^{HN}. \quad (3)$$

The PTT_{ij} term represents the packet transmission time over a link ij , and is calculated by

$$PTT_{ij} = DIFS + DATA + SIFS + ACK, \quad (4)$$

where $DIFS$ and $SIFS$ are the inter-frame spacing used in the MAC layer, $DATA$ is the data frame transmission time defined as the ratio of data frame size and link data rate (i.e., Link data rate is the median value of all used data rates over a specific link within a window of one second), and ACK is the acknowledgment frame transmission time defined as the ratio ACK frame size and the basic data rate (e.g., 1 Mbps for 802.11b). On the other hand, Col_{ij}^{HN} represents the expected number of collisions on link ij caused by the set of all the hidden links for link ij .

Col_{ij}^{HN} is estimated using an analytical model based on the assumptions similar to the ones used in [3], where the collisions caused by nodes within the CS_{range} are negligible since CSMA will prevent such cases. Moreover, each node generates packets in a saturated manner, i.e., a node always has packets to send, and RTS/CTS is turned off. The analytical model for Col_{ij}^{HN} can be illustrated using a four node chain as in Path-1 of Fig. 1 with a single channel, where link cd is a hidden link for link ab , and node b is a CSN for both node a and node c .

In order to estimate the number of retransmissions caused by a HL for a packet, a time interval, $T_{interval}$, is considered for nodes within the CS_{range} of node i , and it contains nodes transmission time, idle time, collisions time, and waiting time for the end of other nodes transmission (i.e., in our protocol $T_{interval}$ is set to one second). Let TX_i^{time} is the time spent by node i in packet transmission over a channel during $T_{interval}$. TX^{time} can be for one packet or a number of successive packets including their retransmissions, but excluding the back-off count down, because other nodes TX^{time} can reflect that. TX^{time} is monitored during run time at MAC layer, which means it reflects the variation in used packet sizes and data rates. Based on this, node's i transmission ratio over a channel (TX_i^{ratio}) is $TX_i^{time} / T_{interval}$.

Collisions due to HNs within b 's $T_{interval}$ will occur only when transmissions over links ab and cd overlap in time. Furthermore, if there are any active CSNs for node a , then

node a will not be able to transmit over link ab , hence, no collisions due to HNs. Similarly, while node b is transmitting over link bc , neither node a nor node c will be able to transmit over links ab and cd , respectively. Therefore, to estimate the *vulnerable period* (VP) where collisions over link ab may happen due to link cd , the time during which both AffL ab and HL cd are idle due to CSNs transmission during a 's $T_{interval}$, and c 's $T_{interval}$, respectively, should be estimated. The estimated idle time ratio for both links should be then excluded from b 's $T_{interval}$.

The link idle time *ratio* for the AffL ij ($AFL^{Idle}(ch_n)$) due to transmissions over links within the CS_{range} of link ij during $T_{interval}$ is estimated as $(1 - TX_i^{ratio})$. Since link ij is either in transmitting or idle mode, and TX_i^{ratio} estimation considers the variation in transmission time interval due to used packet sizes and data rates variation, then excluding TX_i^{ratio} from $T_{interval}$ to calculate the *ratio* time during which a node is idle, is a reasonably accurate measure. The same idle time *ratio* estimation applies for HL fg ($HNL_{fg}^{Idle}(ch_n)$), which is $(1 - TX_f^{ratio})$. Since AffL and HL transmissions are independent, the time during which *both* the AffL ij and the HL fg remain idle, $AfHn^{Idle}$, is estimated as:

$$AfHn^{Idle}(ch_n) = (AFL_{ij}^{Idle}(ch_n) \times HNL_{fg}^{Idle}(ch_n)). \quad (5)$$

The above equation works only when link ij has one HL, therefore, different HNL^{Idle} estimation is needed in the case of multiple HNs. In order to estimate the time *ratio* during which none of the HNs are transmitting, two cases should be considered: First, HNs are inside each others CS_{range} . In this case the HNs transmissions are disjoint, therefore, their idle time *ratio* is estimated as follows:

$$HNL_{CSIn}^{Idle}(ch_n) = 1 - \sum_{kl \in HL_{ij,fg}^{CS}} TX_{kl}^{ratio}. \quad (6)$$

where the $HNL_{CSIn}^{Idle}(ch_n)$ is the fraction of air time were all hidden links that use channel n and reside within each other's CS_{range} are idle. $HL_{ij,fg}^{CS}$ is the set of HNs for link ij and they reside within the CS_{range} of link fg . Second, HNs are outside each others CS_{range} . In this case HNs transmissions are independent, therefore, their idle time is estimated as follows:

$$HNL_{CSOut}^{Idle}(ch_n) = \prod_{kl \in HNL_{ij}} (1 - TX_{kl}^{ratio}). \quad (7)$$

where the $HNL_{CSOut}^{Idle}(ch_n)$ is the fraction of air time were all hidden links that use channel n and reside outside each other's CS_{range} are idle. HNL_{ij} is the set of HNs for link ij and they reside outside each other's CS_{range} . Based on the above two equations, the HNL^{Idle} value is estimated as follows:

$$HNL^{Idle}(ch_n) = \prod_{fg \in HNL_{ij}} (1 - \sum_{kl \in HL_{ij,fg}^{CS}} TX_{kl}^{ratio}). \quad (8)$$

The *vulnerable period* (VP) when collision may occur over link ij due to the hidden link fg can be calculated as follows:

$$VP = 1 - AfHn^{Idle}(ch_n). \quad (9)$$

In order to predict how many collisions will occur over link ij , the fraction of time of HN's TX^{ratio} during VP is estimated. However, in the case of multiple HNs, variant HN's TX^{ratio} s should be considered to reflect the variant effect of

variant packet sizes and data rates over the estimated number of collisions. Therefore, the maximum HN's TX^{ratio} value is considered ($\max_{fg \in HL_{ij}} \{TX_{fg}^{ratio}\}$). This is represented by the probability of collisions over link ij due to one or multiple hidden links, $P(Col_{ij}^{HN})$, given as:

$$P(Col_{ij}^{HN}) = \frac{(\max_{fg \in HL_{ij}} \{TX_{fg}^{ratio}\})}{VP} \times PTT'_{ij}, \quad (10)$$

where HL_{ij} is the set of HNs for link ij and PTT' is the effective PTT when collisions can occur over link ij , and represents the time ratio used by $DATA$ frame transmission over AffL ij , $\frac{DATA_{ij}}{PTT_{ij}}$, since no collisions can occur during ACK frame transmission as it has already been proven in [3]. Finally, the expected number of collisions due to hidden nodes is given as

$$Col_{ij}^{HN} = \frac{1}{1 - P(Col_{ij}^{HN})}. \quad (11)$$

It is important to note that the purpose of Col_{ij}^{HN} is to provide *relative* rather than absolute values. We definitely do not contest the value of more complicated models in general; we do however provide an example where a simple model can perform effectively as our simulation results shows in Sec. 6. This all come as a part of our goal to ensure that our model remains simple enough to be utilized as a handy model for a routing metric with minimal control packet overhead. One factor that was not considered is the capture effect [18], which also has an impact on the collision probabilities, which will be considered in our future work.

4.2 Weighted CEPTT with Carrier Sense Interference ($WCEPT^{CS}$)

$WCEPT^{CS}$ is an enhanced WCETT metric that consider both inter-flow and intra-flow interference, uses a modified ETX (METX) to better reflect dynamic changes in link quality, and improves WCETT channel diversity recognition. It is given by:

$$WCEPT^{CS} = (1 - \alpha) \times \left(\sum_{uv \in CS_p} EPTT_{ij}^{CS} \right) + \alpha \times \max_{ij, uv \in p} \left\{ \sum_{uv \in CSLp_{ij}(ch_n)} EPTT_{uv}^{CS}(ch_n) \right\}, \quad (12)$$

where α is a tunable parameter ($0 \leq \alpha \leq 1$). The first term represents the total time needed to transmit a packet over path p , including retransmissions and the waiting time spent to seize the medium. $EPTT_{ij}^{CS}$ is the expected packet transmission time over link ij including retransmissions, and CS_p represents the union set of carrier sense links for each link ij in path p , regardless of whether these carrier sense links are in the path p itself or adjacent to it. CS_p considers the effects of both intra-flow and inter-flow interference and is given by

$$CS_p = \bigcup_{ij \in p} CSLp_{ij}(ch_n), \quad (13)$$

where $CSLp_{ij}(ch_n)$ is the set of links residing within the carrier sense range of link ij using channel n including link ij itself. The second part of Eq. (12) represents the *bottleneck channel* over path p , which allows for recognition of paths with better channel diversity. $EPTT_{uv}^{CS}$ is the expected packet transmission time of link uv , which is a CS

link for link ij using the same channel, and both links are on the path p . The bottleneck channel is the largest among $EPTT_{uv}^{CS}$ summations for links using the same channel and residing in one another's carrier sense range. $EPTT_{ij}^{CS}$ is defined as

$$EPTT_{ij}^{CS} = METX_{ij}(ch_n) \times PTT_{ij}, \quad (14)$$

where $METX_{ij}(ch_n)$ is the *modified ETX* for link ij operating on channel n , and is given by

$$METX_{ij} = \frac{1}{wDR_f \times wDR_r}, \quad (15)$$

where $METX_{ij}$ is the estimated number of retransmissions a packet may suffer including the original transmission (i.e., bounded by the maximum retry limit at MAC layer) over link ij . To better reflect dynamic changes in link quality, $METX$ value is updated every second using wDR_f and wDR_r , which are the *weighted forward* and *reverse delivery ratios* over link ij , respectively. These are estimated every second using a moving averaging technique to smooth delivery ratios during and between sample periods as follows:

$$wDR_{f,r} = (1 - \lambda) \times newDR_{f,r} + \lambda \times oldDR_{f,r}, \quad (16)$$

where λ is a smoothing factor ($0 < \lambda < 1$) and $newDR_{f,r}$ and $oldDR_{f,r}$ represent the new and old delivery ratios, respectively. At the beginning of a sample period, $newDR_{f,r}$ is set to 1, then every second during the sampling period the $newDR_{f,r}$ is estimated as follows:

$$newDR_{f,r} = 1 - \frac{accum_pkt}{retrans_{max} + 1}, \quad (17)$$

where $accum_pkt$ is the number of lost Hello packets accumulated until the current second within the sampling period, window of $retrans_{max} + 1$ seconds, which equals the number of maximum retransmissions in MAC layer added to the original transmissions. This window is used to serve as a normalization factor to prevent saturation of the $METX$ value. In our metric, λ is set to 0.2 so that $newDR$ is given a higher weight than the old one.

5. HIAM-BASED ROUTING PROTOCOL

This section proposes a HIAM-based routing protocol. Although HIAM can be applied to any routing protocol, AODV [19] is used as a case study. In the case study, the maximum hop count metric in AODV is replaced with HIAM and some of the AODV control packets are extended to accommodate parameters needed for HIAM. Each node maintains a Direct Table and an Indirect Table to obtain all the information needed to identify its CSLs and HLs. A node's *Direct Table* includes information about neighbor nodes residing within its transmission and CS_{range} (direct neighbor), while an *Indirect Table* includes information about neighbors of direct neighbors (i.e., usually two hops away nodes). An example of entry formats for Direct Table, Indirect Table, and Hello and RREQ packets are shown in Fig. 3. The entries example is based on the network topology shown in Fig. 4.

A Direct Table entry represents the link information between a node and one of its direct neighbor node and consists of the following fields: **Daddr** is the address of a direct neighbor node; **ChID** is the channel used to communicate with a direct neighbor node; **TX^{ratio}** is the transmission time ratio of a direct neighbor on a channel; **EPTT^{CS}** is the expected

Dest_addr	Src_addr	Format of a Direct_table entry							
4 bytes	4 bytes	Daddr	ChID	TX ^{ratio}	EPTT ^{CS}	wDR _r	CSr	ST	
		4 bytes	2 bits	1 byte	4 bytes	6 bytes	1 bit	1 bit	
	node C	D	Ch 1	D TX ^{ratio}	CD EPTT ^{CS}	CD wDR _r	D's CSr = 0	D ST	
		B	Ch 2	B TX ^{ratio}	CB EPTT ^{CS}	CB wDR _r	B's CSr = 0	B ST	
		F	Ch 1	F TX ^{ratio}	CF EPTT ^{CS}	CF wDR _r	F's CSr = 0	B ST	
		A	Ch 2	A TX ^{ratio}	CA EPTT ^{CS}	CA wDR _r	A's CSr = 1	A ST	
		G	ch2	G TX ^{ratio}	CG EPTT ^{CS}	CG wDR _r	G's CSr = 1	G ST	

i – Format of Hello Packet (Node C's Hello packet & Direct Table)

Daddr	Iaddr	ICHID	ITX ^{ratio}	EPTT ^{CS}	AfHn ^{idle}	ICSr	IST
4 bytes	4 bytes	2 bits	1 byte	4 bytes	4 bytes	1 bit	1 bit
C	D	Ch 1	D TX ^{ratio}	CD EPTT ^{CS}	----	D's CSr = 0	D ST
C	B	Ch 2	B TX ^{ratio}	CB EPTT ^{CS}	----	B's CSr = 0	B ST
C	F	Ch 1	F TX ^{ratio}	CF EPTT ^{CS}	----	F's CSr = 0	F ST
C	A	Ch 2	A TX ^{ratio}	CA EPTT ^{CS}	----	A's CSr = 1	A ST
C	G	Ch 2	G TX ^{ratio}	CG EPTT ^{CS}	----	G's CSr = 1	G ST
A	B	Ch 1	B TX ^{ratio}	AB EPTT ^{CS}	AB AfHn ^{idle}	B's CSr = 0	B ST
A	C	Ch 2	C TX ^{ratio}	AC EPTT ^{CS}	----	C's CSr = 1	C ST

ii – Format of an Indirect Table entry (Node B's Indirect Table)

Daddr	ChID	TX ^{ratio}	EPTT ^{CS}	wDR _r	CSr	ST
4 bytes	2 bits	1 byte	4 bytes	4 bytes	1 bit	1 bit
A	Ch 1	A's TX ^{ratio}	BA EPTT ^{CS}	BA wDR _r	A's CSr = 0	A ST
C	Ch 2	C TX ^{ratio}	BC EPTT ^{CS}	BC wDR _r	C's CSr = 0	C ST
D	Ch 2	D TX ^{ratio}	BD EPTT ^{CS}	BD wDR _r	D's CSr = 1	D ST
F	Ch 2	F TX ^{ratio}	BF EPTT ^{CS}	BF wDR _r	F's CSr = 1	F ST
G	Ch 2	G TX ^{ratio}	BG EPTT ^{CS}	BG wDR _r	G's CSr = 1	G ST

iii – Format of a Direct Table entry (Node B's Direct Table)

Src.&Dst. addr	Src.&Dst. Seq. No.	Faddr	ChID	EPTT ^{CS}	sumEPTT ^{CS}	BW	AfHn ^{idle}	HN ^{max} (TX ^{ratio})
8 bytes	8 bytes	4 bytes	2 bits	4 bytes	4 bytes	1 byte	2 bytes	2 bytes
		A	Ch 1	AB EPTT ^{CS}	AB sumEPTT ^{CS}	AB BW	AB AfHn ^{idle}	AB HN ^{max} (TX ^{ratio})
		B	Ch 2	BC EPTT ^{CS}	BC sumEPTT ^{CS}	BC BW	-----	-----

iv – Format of a RREQ Packet (RREQ packet arrived at Node C from Node B)

Figure 3: Illustration of data exchange among Direct Table, Indirect Table, and RREQ.

packet transmission time with respect to CSI between the node and a direct neighbor node (see Eq. (14)); wDR_r is the weighted reverse delivery ratio representing its link quality (see Eq. (16)); **CSr** is a flag that indicates whether a direct neighbor node is out of the node's TX_{range} but still within the node's CS_{range} ; **ST** is a flag that indicates whether this link is idle or active in sending/receiving data packets within a given time interval. This time interval is configured based on inter-arrival times of data packets.

An Indirect Table is constructed and updated based on Direct Table information included in Hello packets received from direct neighbors as shown in Fig. 3-i and 3-ii. Each node uses this table to find its HLs and to estimate collision probability caused by them. A node's Indirect Table entry represents link information between its direct and indirect neighbors, and consists of the following fields: **Daddr**, **Iaddr**, **ICHID**, **ITX^{ratio}**, **EPTT^{CS}**, **ICSr**, and **IST**. All fields except **AfHn^{idle}** have identical meanings as in Direct Table.

Iaddr and **ICSr** are used to identify HNs. **ITX^{ratio}** is used together with **ICHID** and **ICSr** to determine the first two terms in Eq. (5). This leads to the calculation of VP in Eq. (9), which is then used to determine Col_{ij}^{HN} in Eq. (11). Note that not all HNs can be identified based only on indirect neighbor nodes. Therefore, these HNs are identified during the Route Discovery stage (see Sec. 5.3), and used to determine the final value of Col_{ij}^{HN} and $EPTT_{ij}^{HN}$ in Eq. (3).

In addition to the two tables, RREQ packets, which are used to establish routes, require additional fields to process HIAM. The format of the RREQ packet shown in Fig. 3-iv contains the usual source address (**Src_addr**) and destination address (**Dst_addr**), and their sequence numbers. In addition, it contains the following fields: **Faddr** is the previous hop address; **ChID** is the channel used by the previous hop node to forward RREQ packet to the current node; **EPTT^{CS}**

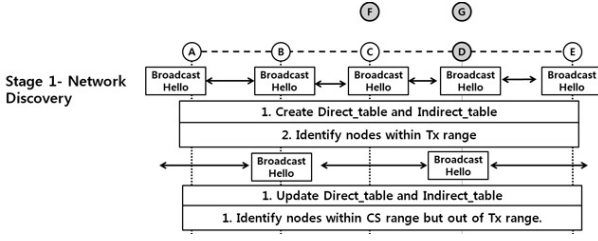


Figure 4: Stage 1 - Network Discovery.

is used by each node to locally determined the bottleneck channel (the second term in Eq. (12)) of the path traversed by RREQ; $\text{sumEPPT}^{\text{CS}}$ is the summation of all the EPTT^{CS} values for the path traversed by RREQ, excluding the shared CSLs with the previous hop(s); $\text{AfHn}^{\text{Idle}}$ is the product of AffN idle time and HNs idle time; $\text{HN}^{\text{max}}(\text{TX}^{\text{ratio}})$ is the highest HN TX^{ratio} between a number of HNs; BW , is the link bandwidth.

The HIAM-based routing protocol consists of three stages: Network Discovery, Exchanging Periodic Hello Packets, and Route Discovery. The following subsections discuss the three stages using the network topology illustrated in Fig. 4 with Txrange of 370m, and CSrange of 670m, and the distance between nodes is 300m. The data exchange between tables in each stage is shown in Fig. 3.

5.1 Stage 1 - Network Discovery

This stage is illustrated in Fig. 4. During the first five seconds of the network initialization, Hello packets are exchanged in succession, one with the default *transmission power* (TX_{pw}) and another with the *CS power* (CS_{pw}). CS_{pw} represents the transmission power needed to reach nodes within the CSrange and is higher than the *CS threshold* (CS_{thr}) as shown in Fig. 4. This allows each node to *identify all the nodes that are within its CSrange but out of its Txrange* . For example, using our mechanism node B can identify that both nodes A and C are within its Txrange , while nodes D, F, and G are within its CSrange . However, without our mechanism node B cannot recognize that nodes D, F, and G are neighbors and it will mistakenly assume that node C is a hidden node for node A, since node C is within the Txrange of node B but not for node A. This is a problem that existing work [9, 10] suffer from when applied in networks with unequal transmission and CS ranges, due to discovering and exchanging lists of neighbors within Txrange only.

Each node then constructs the Direct Table based on the received Hello packets and mark each node (i.e., using the CSR field in Direct Table) based on its identified range as shown in Fig. 3. The time difference between the two broadcasts of Hello packets should be large enough to ensure that every node will receive these packets. Due to the stationary nature of nodes within mesh networks, the Network Discovery stage can be done once or the Hello packets can be transmitted using CS_{pw} once every a period of time, after waiting for silent safe guard period of 5 ms to account for time differences between nodes and to prevent colliding with traffic. This allows our routing protocol to work with variant Txrange and CSrange , and identify interfering links better than the hop-distance-based interference model [16].

5.2 Stage 2 - Exchanging Periodic Hello packets

During this stage, each node periodically broadcasts Hello packets with TX_{pw} to (1) obtain the necessary information for Direct Table and Indirect Table and (2) identify hidden links. Based on the received Hello packets, nodes B in Fig. 4 performs the following steps (similar operations are also performed by *all nodes*):

1. Update Direct Table - Node B checks its Direct Table to see if the link information exists for both nodes A and C. If so, the corresponding TX^{ratio} and ST field are updated. Otherwise, two new entries are created in the Direct Table, one with Daddr of node A and ChID of link BA and the other with Daddr of node C and ChID of link BC as shown in Fig. 3-iii;
2. Update Indirect Table - Node B updates its Indirect Table based on the received Direct Table information from nodes A and C as shown in Fig. 3-ii;
3. Calculate wDR_r , METX and EPTT^{CS} - Node B re-calculates wDR_r values in the Direct Table for links BA and BC based on the number of received Hello packets from nodes A and C. In addition, node B retrieves wDR_r values for links BA and BC from the received Hello packets, which are the wDR_r values corresponding to links AB and CB in the Hello packet, respectively, as shown in Fig. 3-i. Then, node B calculates METX and then EPTT^{CS} for both links BA and BC and records the EPTT^{CS} value in its Direct Table. The updated Direct Table is then included in the Hello packet and broadcasted; and
4. Identify hidden links - Node B identifies the HNs for node A by comparing the direct neighbors of both node B and node A. If direct neighbors of node B are not direct neighbors of node A, then they are considered as HN candidates for node A (i.e., HNs are node D, F, and G). For each one of these candidates, links that are active and use the same channel as link AB are considered as HLs. This information is then used to calculate $\text{AfHn}^{\text{Idle}}$ (i.e., Eq. (5)) for the corresponding entry in the Indirect Table, as shown in Fig. 3-ii.

However, if HNs are within the CSrange but outside the Txrange of node B, and they are more than two hops away from node B (i.e., like node G), then it will not have all the information needed to identify the HNs. This is because the Indirect Table provide information about nodes that are two hops away, and Hello packets from such HNs will not reach node B much often, which makes their information stale. Therefore, HLs in such cases will need to be identified during the Route Discovery Phase by intermediate nodes like node C or node D as discussed in Sec. 5.3.

In addition, the size of the Hello packets significantly increases as the numbers of nodes and channels increase. This in turn increases the control packet overhead and wastes network bandwidth. Therefore, Hello packets broadcasting is modified using a *grouping method*, where the entries in the Direct Table are subdivided into groups based on ChID . Each group of records is then placed in a separate Hello packet and broadcast only on the channel that matches its ChID . This approach significantly reduces the broadcasting overhead in multi-channel environments.

5.3 Stage 3 - Route Discovery

The Route Discovery procedure is discussed based on the assumption that in Fig. 4 node A is the source and node E is the destination. The following steps are performed when node C receives a RREQ from node B :

1. Update RREQ packet - $EPTT^{CS}$ values stored in RREQ are used to locally determine the bottleneck channel of the path RREQ passed through. The previous hop address (i.e., node B) and channel is used to retrieve link BC corresponding $EPTT^{CS}$ value from the Indirect Table. This value is used to update link BC 's $EPTT^{CS}$ field in RREQ, $sumEPTT^{CS}$ for the path, and BW value after extracting it from B 's $EPTT^{CS}$ value, as shown in Fig. 3-iv. Finally, $Faddr$ and $IChID$ fields of RREQ are overwritten with B 's address and channel.
2. Identify new hidden links and calculate $AfHn^{Idle}$ - The following two cases can occur when identifying HNs: First, node C is identified as a HN but it has been idle for more than 1 second, which means it was not identified as a HN in Stage 2. To check if this case applies to node C , node C is a hidden node for node A if A 's address in $Faddr$ and $ChID$ from the RREQ matches $Iaddr$ and $IChID$ of the Indirect Table entry obtained using the address of node B , and if node A is not a (i.e., $Daddr$) of node C . In our example node C is not a HN but node D is, therefore, when the RREQ reaches to node D it should check if there are HNs within its CS_{range} (i.e., nodes $F, G, and D$) for node A , and retrieve their TX^{ratio} values to recalculate $AfHn^{Idle}$ value. Second, node C checks whether there are any other hidden nodes for node A that node B was unable to identify during Stage 2. Such HNs are within the CS_{range} of both node B and node C , and they are $Iaddr$ for node C (i.e., like node G). Node C check its Indirect Table to see if node B (i.e., $Daddr$) have node G (i.e., $Iaddr$) within CS_{range} but out of TX_{range} of node B (i.e., using $ICsr=1$). Then, node C checks its Direct Table to see if node G is within the CS_{range} of node C (i.e., using $Csr=1$). When both of these conditions are satisfied, node G is identified as a HN for node A , and its TX^{ratio} is retrieved by searching node C 's Indirect Table for a $Daddr$ (i.e., like node D) that have node G as $Iaddr$ within its TX_{range} (i.e., $ICsr=0$). After all the HNs are identified, their TX^{ratio} are used to re-calculate (HN^{idle}) in Eq. (8), and find the $HN^{max}(TX^{ratio})$. Finally, the $AfHn^{Idle}$ value stored in the row corresponding to node A 's address in RREQ is updated.
3. Calculate HIAM - Calculate the HIAM value for the path up to this node.
4. Update routing table - If the calculated HIAM value for the path traversed by RREQ is lower than the one already stored in the routing table, then the routing table is updated with the new path and RREQs are forwarded; otherwise, the RREQ packet is dropped. If the number of forwarded RREQ packets is higher than three then any newly received RREQ is dropped. The number of waited RREQ packets is tunable. This scheme is referred to as *early elimination scheme*, and it aims to reduce route discovery overhead.

5. Initiate *Route Reply* (RREP) - RREP is performed by the destination node. In the HIAM-based routing protocol, the destination node will wait for at most three RREQs in a specified time interval. HIAM is calculated for the received RREQs and the path with the lowest value is chosen. The chosen path will be stored in the RREP packet in a reverse order, so that as RREP passes through nodes on its way back to the source, their routing table will be updated based on this path.

6. PERFORMANCE EVALUATION

The QualNet simulator [12] was used to evaluate the performance of HIAM. The simulation environment consists of two network topologies with 802.11a radios. Topology 1 consists of five nodes chain surrounded by a number of nodes that varies between zero to 10 nodes. This topology is used to evaluate the accuracy of our proposed analytical model in the presence of variant number of interfering links. Topology 2 consists of 25 randomly placed nodes. The aim of using such topology is to test the performance of HIAM in a more realistic configuration where the network has a fair number of HNs and CSI. The configuration of Topology 1 consisted of a number of CBR flows that varies between one to nine flows, and were distributed as follows: one flow runs over the five nodes chain, and the rest are distributed over the interfering links. The used flow rate is 1,000 kbps and the simulation time is 100 seconds. The configuration of Topology 2 consisted of 11 CBR flows, and every 100 seconds the sender/receiver pairs are changed. To make the traffic load more diverse a new CBR flow starts every five second until all the 11 CBR flows are running concurrently for the remaining 100 seconds. The same process is repeated every 100 seconds for a total simulation time of 500 seconds. Three different packets sizes have been used concurrently: 160, 500, and 1500 bytes. We used packet sizes that cover four major applications, which are VoIP, file transfer, video streaming, and web surfing. The simulation results are the average of 10 runs with variant sender/receiver pairs for each run; all nodes use three orthogonal channels and three 802.11a radios, and each channel is statically assigned to one radio. The link speed is multi rate, the TX_{pw} is 19 dBm, and CS_{thr} is -83 dBm. HIAM β is 0.8, WCEPTT α is 0.5, and METX λ is 0.2 .

6.1 Simulations Results

Figs. 5 shows the comparison between our analytical model estimation of HN collisions and the actual HN collisions number monitored during simulation. Figs. 5 shows that our model achieves relatively close estimation of HN collisions to the actual ones. The number of estimated collisions decreases as the number of CSLs increases, which matches the trend of the actual HN collisions. Despite any inaccuracies, note that in the plot, we are able to unambiguously distinguish between various path qualities with variant number of CSLs.

Figs. 6-a ~ 6-e compare the performance of HIAM against ETX, WCETT, IRU, and PPTT. Note that the Hidden Node Aware metric [9] was not included in our comparison because it is interrelated with 802.11s and uses many of the 802.11s built in functions and control packets, which is not available in 802.11a/b/g that HIAM is built on. Therefore, a direct comparison was not feasible. Fig. 6-a shows

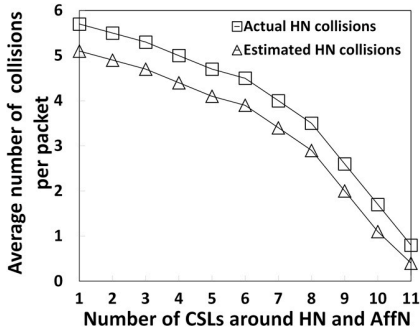


Figure 5: The accuracy of HN collisions estimation.

the average throughput for the random topology. HIAM provides on average 0.47x improvement over PPTT. The reasons for this are four-fold: First, the HN problem is not given the highest priority in the path selection process for PPTT, which may select paths with lower carrier sense interference, but the effect of the hidden nodes is higher than other paths, hence, more dropped packets and broken links; Second, PPTT uses an analytical model to predict the effect of CSI, while HIAM uses active probing that results in much more accurate prediction of current link status; Third, PPTT control packet size grows faster than HIAM Hello packets (i.e., HIAM Hello packet size reaches up to 1.2x smaller than PPTT control packet size), due to Hello packets *grouping method* discussed in Sec. 5.2. Therefore, HIAM wastes less bandwidth and delay than PPTT in control packets broadcast; Fourth, PPTT routing protocol cannot identify all the existing hidden nodes within an environment, especially the ones that are more than two hops away, as discussed in Sec. 5.2, which causes incorrect HN collision estimations, and wrong path selection.

On the other hand, ETX, WCETT and IRU show 0.61x, 0.52x, and 0.49x lower throughput than HIAM, respectively. This is for two reasons: First, they do not explicitly consider the hidden node problem in the path selection process; Second, both WCETT and IRU utilize ETX to capture the frequently changing link quality. However, ETX is unable to accurately capture this behavior due to the large interval used to calculate ETX (usually 10 seconds). In contrast, HIAM uses *METX* (see Eq. (15)), which is updated every second using a moving average.

The throughput improvement achieved by HIAM is further supported by the number of retransmissions, broken links, and dropped packets, as well as the amount of control packet overhead. Moreover, their causes are highly interrelated. Fig. 6-c shows the average number of broken links. As expected, HIAM has significantly lower numbers of broken links than ETX, WCETT, IRU, and PPTT. These results are related with the packet retransmission results shown in Fig. 6-b. That is, a link breakage occurs when the number of retransmissions for a packet exceeds the MAC retry limit, which occurs mostly due to the hidden node problem. Link breakage in turn causes routing instability (as discussed in Sec. 2), increases control packet overhead, and forces all packets destined to that link to be dropped from queues. This is apparent in Fig. 6-d, ETX, WCETT, IRU, and PPTT achieves 12.9x, 9.1x, 7.8x, and 5.3x higher dropped packets more than HIAM.

Fig. 6-f shows the control packet overhead, which is de-

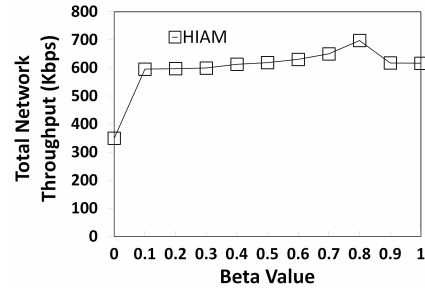


Figure 7: Configuration 3: Topology 2, 802.11b/g. Total network throughput for different β values.

finer as the ratio of total number of RREQ, RREP, and RERR packets compared to the total number of successfully received data packets in bytes. The control overhead values for ETX, WCETT, IRU, and PPTT are significantly higher than HIAM due to their routing instability. They often choose paths with hidden nodes resulting in frequently broken links and a higher number of initiated RERR and RREQ packets, which consequently lead to higher number of RREP packets. Furthermore, these broken links will force them to search for longer paths around the broken links resulting in a higher number of retried RREQ packets.

Fig. 6-e shows that ETX, WCETT, IRU, and PPTT have 1.7x, 2x, 1.24x, and 0.027x higher end-to-end delay than HIAM. This is a direct consequence of high number of retransmissions, and unnecessary route discovery caused by high number of link breakage.

Fig. 7 shows the throughput results for the third configuration. This configuration was run on Topology 2 with 802.11b/g radios with 10 CBR flows, and 0.2 Mbps \sim 3 Mbps flow rates. It is used to analyze the effect of each component of HIAM, i.e., $CEPTT^{HN}$ and $WCEPTT^{CS}$, on the overall throughput when they are considered separately and when they are combined with different β values. In addition, this configuration compares the performance of two versions of $WCEPTT^{CS}$, one with ETX [8], and the other with METX. Fig. 7 shows that disabling $CEPTT^{HN}$ (i.e., $\beta = 0$) caused 79% throughput reduction for HIAM. As β increases, throughput for HIAM increases. However, beyond $\beta = 0.8$, the throughput decreases by 12% because $WCEPTT^{CS}$ is almost disabled, hence, the CSI effect is not considered. Moreover, using METX results in 12% higher throughput than using ETX.

7. CONCLUSION AND FUTURE WORK

Proposed HIAM: it considers both the HN problem and CSI. HIAM specifically considers packet transmission time along a path with respect to collisions caused by HNs. HIAM also reflects the CSI by estimating the packet transmission time along the path with respect to retransmissions caused by the CSI. Our simulation results show that HIAM achieves significantly higher throughput, and routing stability than ETX, WCETT, IRU, and PPTT.

8. ACKNOWLEDGMENT

This work was supported by the National Research Foundation of Korea(NRF) grant funded by the Korea government(MEST) (No. 2012R1A2A2A01008244).

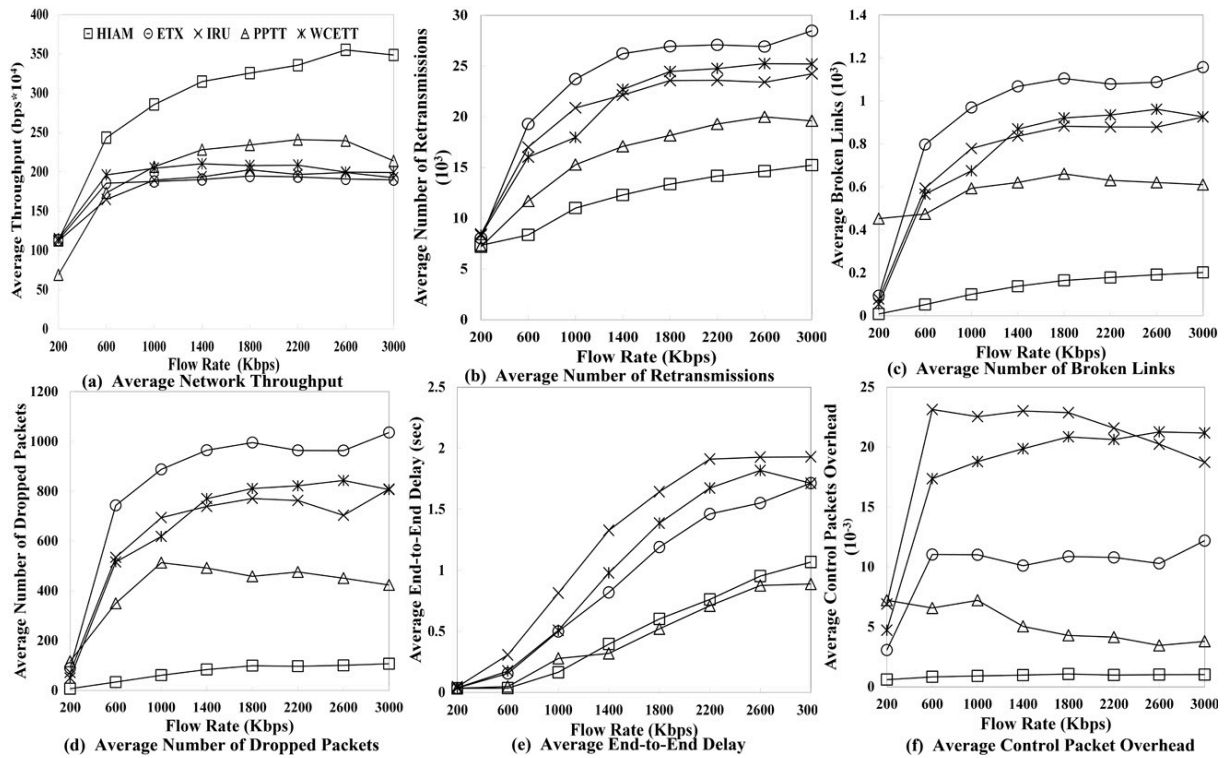


Figure 6: Topology 2 (Random topology) evaluation results, β is 0.8, α is 0.5, and λ is 0.2.

9. REFERENCES

- [1] I.F. Akyildiz, X. Wang, and W. Wang, "Wireless Mesh Networks: A Survey," *Computer Networks and ISDN Systems*, Vol.47, No.4, pp.445-487, 2005.
- [2] J. Li, C. Blake, D.S.J. De Couto, H.I. Lee and R. Morris, "Capacity of Ad hoc Wireless Networks," *Proceedings of ACM MOBICOM*, pp.61-69, 2001.
- [3] P.C. Ng and S.C. Liew, "Throughput Analysis of IEEE 802.11 Multi-hop Ad hoc Networks," *IEEE/ACM TON*, Vol.15, No.2, pp.309-322, April 2007.
- [4] P.C. Ng, S.C. Liew, K.C. Sha, and W.T. To, "Experimental Study of Hidden Node Problem in IEEE 802.11 Wireless Networks," *ACM SIGCOM'05*.
- [5] S. Ray, D. Starobinski, and J. Carruthers, "Performance of Wireless Networks with Hidden Nodes: A Queuing-theoretic Analysis," *Journal of Computer Communications*, 2005.
- [6] L. Tung; W. Shih, T. Cho, Y.S. Sun, and M. Chen, "TCP Throughput Enhancement over Wireless Mesh Networks," *IEEE Communications Magazine*, 2007.
- [7] D. De Couto, D. Aguayo, J. Bicket, and R. Morris, "High-throughput Path Metric for Multi-Hop Wireless Routing," *Proceedings of ACM MOBICOM*, 2003.
- [8] R. Draves, J. Padhye, and B. Zill, "Routing in Multi-radio, Multi-hop Wireless Mesh Networks," *Proceedings of ACM MobiCom*, pp.114-128, 2004.
- [9] J. Sangiamwong and T. Sugiyama, "Hidden Node Problem Aware Routing Metric for Wireless LAN Mesh Networks," *IEEE International Symposium on Personal, Indoor and Mobile Radio Comm.'07*.
- [10] S. Yin, Y. Xiong, Q. Zhang and X. Lin, "Traffic-aware Routing for Real-time Communications in Wireless Multi-hop Networks: Research Articles," *Wireless Communications & Mobile Computing*, 2006.
- [11] G. Parissidis, M. Karaliopoulos, T. Spyropoulos, B. Plattner, "Interference-Aware Routing in Wireless Multihop Networks," *Mobile Computing, IEEE Transactions on*, vol.10, no.5, pp.716-733, 2011.
- [12] The QualNet Network Simulator - <http://www.scalable-networks.com/>
- [13] C. E. Perkins, E. M. Belding-Royer, and S. Das, "Ad hoc On-Demand Distance Vector (AODV) Routing," RFC 3561, 2003.
- [14] IEEE Std 802.11b-1999, Part 11: Wireless LAN Medium Access Control (MAC) and Physical Layer (PHY) specifications: High-speed physical layer extension in the 2.4 GHz band, Supplement to ANSI/IEEE Std 802.11, 1999.
- [15] P. Chatzimisios, A.C. Boucouvalas, and V. Vitsas, "Effectiveness of RTS/CTS handshake in IEEE 802.11a Wireless LANs," *Electronics Letters*, 2004.
- [16] J. Lee, S.J. Lee, W. Kim; D.H. Jo, T. Kwon, and Y. Choi, "RSS-based Carrier Sensing and Interference Estimation in 802.11 Wireless Networks," *IEEE SECON*, pp.491-500, 2007.
- [17] Y. Yang, J. Wang, and R. Kravets, "Load-balanced Routing For Mesh Networks," *ACM MC2R*, 2006.
- [18] S. Razak, V. Kolar, N.B. Abu-Ghazaleh, and K.A. Harras, "How do Wireless Chains Behave? The Impact of MAC Interactions," *ACM/IEEE MSWiM*, 2009.
- [19] J. W. Yang, J. K. Kwon, H. Y. Hwang, and D. K. Sung, "Goodput analysis of a WLAN with hidden nodes under a non-saturated condition," *Wireless Communications, IEEE Transactions on*, 2009.